NASA/CR-2002-211456
ICASE Report No. 2002-6


# New Factorizable Discretizations for the Euler Equations

*Boris Diskin*
*ICASE, Hampton, Virginia*

*James L. Thomas*
*NASA Langley Research Center, Hampton, Virginia*


April 2002

## The NASA STI Program Office . . . in Profile

Since its founding, NASA has been dedicated to the advancement of aeronautics and space science. The NASA Scientific and Technical Information (STI) Program Office plays a key part in helping NASA maintain this important role.

The NASA STI Program Office is operated by Langley Research Center, the lead center for NASA's scientific and technical information. The NASA STI Program Office provides access to the NASA STI Database, the largest collection of aeronautical and space science STI in the world. The Program Office is also NASA's institutional mechanism for disseminating the results of its research and development activities. These results are published by NASA in the NASA STI Report Series, which includes the following report types:

- TECHNICAL PUBLICATION. Reports of completed research or a major significant phase of research that present the results of NASA programs and include extensive data or theoretical analysis. Includes compilations of significant scientific and technical data and information deemed to be of continuing reference value. NASA's counterpart of peer-reviewed formal professional papers, but having less stringent limitations on manuscript length and extent of graphic presentations.

- TECHNICAL MEMORANDUM. Scientific and technical findings that are preliminary or of specialized interest, e.g., quick release reports, working papers, and bibliographies that contain minimal annotation. Does not contain extensive analysis.

- CONTRACTOR REPORT. Scientific and technical findings by NASA-sponsored contractors and grantees.

- CONFERENCE PUBLICATIONS. Collected papers from scientific and technical conferences, symposia, seminars, or other meetings sponsored or cosponsored by NASA.

- SPECIAL PUBLICATION. Scientific, technical, or historical information from NASA programs, projects, and missions, often concerned with subjects having substantial public interest.

- TECHNICAL TRANSLATION. English-language translations of foreign scientific and technical material pertinent to NASA's mission.

Specialized services that complement the STI Program Office's diverse offerings include creating custom thesauri, building customized data bases, organizing and publishing research results . . . even providing videos.

For more information about the NASA STI Program Office, see the following:

- Access the NASA STI Program Home Page at ***http://www.sti.nasa.gov***

- Email your question via the Internet to help@sti.nasa.gov

- Fax your question to the NASA STI Help Desk at (301) 621-0134

- Telephone the NASA STI Help Desk at (301) 621-0390

- Write to:
  NASA STI Help Desk
  NASA Center for AeroSpace Information
  7121 Standard Drive
  Hanover, MD 21076-1320

NASA/CR-2002-211456
ICASE Report No. 2002-6


# New Factorizable Discretizations for the Euler Equations

*Boris Diskin*
*ICASE, Hampton, Virginia*

*James L. Thomas*
*NASA Langley Research Center, Hampton, Virginia*

*ICASE*
*NASA Langley Research Center*
*Hampton, Virginia*

*Operated by Universities Space Research Association*


Prepared for Langley Research Center
under Contract NAS1-97046

April 2002

Available from the following:

NASA Center for AeroSpace Information (CASI)
7121 Standard Drive
Hanover, MD 21076-1320
(301) 621-0390

National Technical Information Service (NTIS)
5285 Port Royal Road
Springfield, VA 22161-2171
(703) 487-4650

# NEW FACTORIZABLE DISCRETIZATIONS FOR THE EULER EQUATIONS

BORIS DISKIN* AND JAMES L. THOMAS†

**Abstract.** A multigrid method is defined as having textbook multigrid efficiency (TME) if solutions to the governing system of equations are attained in a computational work that is a small (less than 10) multiple of the operation count in one target-grid residual evaluation. A way to achieve TME for the Euler and Navier-Stokes equations is to apply the distributed relaxation method thereby separating the elliptic and hyperbolic partitions of the equations. Design of a distributed relaxation scheme can be significantly simplified if the target discretization possesses two properties: (1) factorizability and (2) consistent approximations for the separate factors. The first property implies that the discrete system determinant can be represented as a product of discrete factors, each of them approximating a corresponding factor of the determinant of the differential equations. The second property requires that the discrete factors reflect the physical anisotropies, be stable, and be easily solvable.

In this paper, discrete schemes for the nonconservative Euler equations possessing properties (1) and (2) have been derived and analyzed. The accuracy of these scheme has been tested for subsonic flow regimes and is comparable with the accuracy of standard schemes. TME has been demonstrated in solving fully subsonic quasi-one-dimensional flow in a convergent/divergent channel.

**Key words.** Euler equations, textbook multigrid efficiency, distributed relaxation, factorizable schemes

**Subject classification.** Applied and Numerical Mathematics

**1. Introduction.** Full multigrid (FMG) algorithms [3, 4, 13, 22, 26, 27] are the fastest solvers for elliptic problems. These algorithms can solve a general discretized elliptic problem to the discretization accuracy in a computational work that is a small (less than 10) multiple of the operation count in one target-grid residual evaluation. Such efficiency is known as textbook multigrid efficiency (TME) [5, 6]. Extending TME to solutions of the Navier-Stokes equations is a challenging task because the Navier-Stokes equations form a system of coupled nonlinear equations that is not fully elliptic, even for fully subsonic flow, but contains hyperbolic partitions. TME for the Navier-Stokes simulations can be achieved if the different factors contributing to the system could be separated and treated optimally, e.g., by multigrid for elliptic factors and by downstream marching for hyperbolic factors. One of the ways to separate the factors is the *distributed relaxation* method proposed in [3, 4]. The general framework for achieving TME in large-scale computational fluid dynamics (CFD) applications has been discussed in [9, 25].

The major difficulty in efficiently solving the Navier-Stokes equations is encountered with the inviscid (Euler) subset; thus we restrict ourselves to the Euler equations here. The approach to the solution of the Euler equations motivating this paper is based on an FMG algorithm with multigrid cycles employing distributed relaxation. It is envisioned that the FMG-1 algorithm (an FMG algorithm with one multigrid cycle per level) will provide solutions with algebraic error below the level of the discretization error. Another useful characteristic of the solution process is the possibility to rapidly converge residuals to the machine zero.

*ICASE, Mail Stop 132C, NASA Langley Research Center, Hampton, Virginia 23681 (email: bdiskin@icase.edu). This research was supported by the National Aeronautics and Space Administration under NASA Contract No. NAS1-97046 while the author was in residence at ICASE, NASA Langley Research Center, Hampton, Virginia 23681

†Computational Modeling and Simulation Branch, Mail Stop 128, NASA Langley Research Center, Hampton, VA 23681 (email: j.l.thomas@larc.nasa.gov).

The latter property is not necessary for achieving TME, but it is highly favored in practical applications.

The distributed relaxation approach relies on a *principal* linearization of the governing system of nonlinear equations. The principal linearization is derived from the full Newton linearization by removing some unimportant (subprincipal) terms. The principal terms of a linear *scalar* equation are the terms that make major contributions to the residual per a unit change in the solution variable. The principal terms thus generally depend on the scale, or mesh size, of interest. For example, the discretized highest derivative terms are principal on grids with small enough mesh size. For a discretized *system* of differential equations, the principal terms are those that contribute to the principal terms of the *determinant* of the matrix operator.

Design of a distributed relaxation scheme for the Euler equations can be significantly simplified if the target discretization possesses two properties:

(1) The principal linearization of the target discrete system is *factorizable* [4, 5, 6, 19, 20], i.e., the discrete system determinant can be represented as a product of discrete scalar factors, each of them approximating a corresponding factor of the determinant of the *differential* equations.

(2) The obtained scalar factor discretizations reflect the physical anisotropies and are stable and easily solvable.

The main subject of this paper is derivation of new discrete schemes for the nonconservative Euler equations possessing properties (1) and (2). Corresponding conservative discrete schemes and distributed relaxation for them have been considered in [15].

Properties (1) and (2) are automatically obtained with *staggered-grid* discretizations for incompressible and slightly compressible flow. Textbook efficient multigrid solvers employing factorizable staggered-grid discretizations of the *nonconservative* formulations and distributed relaxation have already been demonstrated for high-Reynolds-number viscous incompressible [11, 24] and subsonic compressible [23] flow regimes.

Factorizable schemes for the conservative Euler equations on *collocated* grids have been derived and implemented in [17, 18, 19, 20, 21]. The multigrid solvers in these references employed Collective Gauss-Seidel rather than distributed relaxation. The subsonic-flow convergence rates observed in multigrid V cycles were quite fast (about 0.3 per cycle), far overcoming the theoretical limit for nonfactorizable schemes, and were only slightly grid dependent. However, these rates are still not fast enough to guarantee convergence in an FMG-1 algorithm. The rates also deteriorate somewhat in transonic and supersonic computations and for grids with high aspect ratios. These facts emphasize the need to employ distributed relaxation.

This paper explores new collocated-grid schemes for the compressible Euler equations that satisfy properties (1) and (2) in multiple dimensions. A typical difficulty associated with this type of scheme is a poor measure of $h$-ellipticity (stability) in the discrete approximation for the full-potential factor of the system determinant. By definition (see [2, 4, 26]), a discrete scalar (not necessarily elliptic) operator $L[u]$ possesses a good measure of $h$-ellipticity, if the absolute value of its symbol $|L(\mathbf{w})|$ is well separated from zero for all high-frequency Fourier modes. The operator symbol is defined as the operator response on a discrete Fourier mode: $L[e^{i(\mathbf{w}\cdot\mathbf{j})}] = L(\mathbf{w})e^{i(\mathbf{w}\cdot\mathbf{j})}$, where $\mathbf{j} = (j_x, j_y, j_z)$ are the grid indexes and $\mathbf{w} = (\omega_x, \omega_y, \omega_z), 0 \le |\omega_x|, |\omega_y|, |\omega_z| \le \pi$ are normalized Fourier frequencies. For elliptic operators, high-frequency Fourier modes are the modes satisfying $\max(|\omega_x|, |\omega_y|, |\omega_z|) \ge \pi/2$; for nonelliptic operators, high-frequency Fourier modes are those oscillating in the characteristic directions.

Lack of $h$-ellipticity often implies inefficient relaxation (i.e., a poor smoothing factor for some high-frequency error components) and slow convergence rates in multigrid cycles. Several approaches to overcome the difficulty (mainly in applications to incompressible flow equations) have been proposed (e.g., [1, 10]). Some of the approaches are associated with introduction of additional terms increasing the measure of

$h$-ellipticity, others with averaging spurious oscillations.

The factorizable schemes for multidimensional compressible flow equations proposed in this paper include a mechanism to improve the $h$-ellipticity measure by obtaining *any* desired discretizations for the full-potential factor. TME with an FMG solver employing the distributed relaxation method has been demonstrated for two schemes approximating the Euler equations for a quasi-one-dimensional subsonic flow in a convergent/divergent channel.

The paper is organized as follows: The Euler equations for inviscid compressible flow problems are defined in Section 2. The idea of distributed relaxation is briefly explained in Section 3. Section 4 presents the derivation of the new factorizable schemes for the Euler equations. A model problem, the one-dimensional subsonic Euler equations, is presented in Section 5 together with a comparative analysis of linear discretization schemes. Description of the multigrid solver ingredients is in Section 6 followed by results of nonlinear numerical tests with a subsonic flow in a convergent/divergent channel reported in Section 7. Section 8 contains concluding remarks.

**2. Euler Equations.** The steady-state three-dimensional Euler system of compressible flow equations can be written as

$$\mathbf{R}(\mathbf{q}) \equiv \begin{cases} u\partial_x u + v\partial_y u + w\partial_z u + \frac{1}{\rho}\partial_x p & = 0, \\ u\partial_x v + v\partial_y v + w\partial_z v + \frac{1}{\rho}\partial_y p & = 0, \\ u\partial_x w + v\partial_y w + w\partial_z w + \frac{1}{\rho}\partial_z p & = 0, \\ \rho c^2\partial_x u + \rho c^2\partial_y v + \rho c^2\partial_z w + u\partial_x p + v\partial_y p + w\partial_z p & = 0, \\ \frac{c^2}{\gamma}\partial_x u + \frac{c^2}{\gamma}\partial_y v + \frac{c^2}{\gamma}\partial_z w + u\partial_x \epsilon + v\partial_y \epsilon + w\partial_z \epsilon & = 0. \end{cases} \tag{2.1}$$

where the primitive variables, $\mathbf{q} = (u, v, w, p, \epsilon)^T$, represent velocity, pressure, and internal energy, and are related to the density, $\rho$, and the speed of sound, $c$, through the following equations:

$$p = (\gamma - 1)\rho\epsilon, \tag{2.2}$$

$$c^2 = \gamma p/\rho, \tag{2.3}$$

where $\gamma$ is the ratio of specific heats.

In an iterative (quasi-Newton) procedure, the correction $\delta\mathbf{q} = \mathbf{q}^{n+1} - \mathbf{q}^n$, where $n$ is an iteration counter, can be computed from the equation

$$\mathbf{L}\,\delta\mathbf{q} \;=\; -\mathbf{R}(\mathbf{q}), \tag{2.4}$$

where $\mathbf{L}$ is the principal linearization of the operator $\mathbf{R}(\mathbf{q})$. Thus,

$$\mathbf{L} = \begin{bmatrix} Q & 0 & 0 & \frac{1}{\rho}\partial_x & 0 \\ 0 & Q & 0 & \frac{1}{\rho}\partial_y & 0 \\ 0 & 0 & Q & \frac{1}{\rho}\partial_z & 0 \\ \rho c^2\partial_x & \rho c^2\partial_y & \rho c^2\partial_z & Q & 0 \\ \frac{c^2}{\gamma}\partial_x & \frac{c^2}{\gamma}\partial_y & \frac{c^2}{\gamma}\partial_z & 0 & Q \end{bmatrix}, \tag{2.5}$$

where $Q = \bar{u}\partial_x + \bar{v}\partial_y + \bar{w}\partial_z = (\bar{\mathbf{u}} \cdot \nabla)$, and the coefficients $\bar{\mathbf{u}} = (\bar{u}, \bar{v}, \bar{w})$, $\rho$, and $c^2$ are evaluated from the approximation $\mathbf{q}^n$ and, for the current iteration, are considered as constants unrelated to the target primitive

variables. The determinant of the matrix operator $\mathbf{L}$ is

$$Q^3 \left[ Q^2 - c^2 \triangle \right], \tag{2.6}$$

where $\triangle$ is the Laplace operator. The convection operators, $Q$, and the full-potential operator, $Q^2 - c^2\triangle$, represent hyperbolic and elliptic partitions of the Euler equations.

**3. Distributed Relaxation.** The distributed relaxation method for the Euler equations replaces $\delta\mathbf{q}$ in (2.4) by $\mathbf{M}\,\delta\mathbf{w}$, where

$$\mathbf{M} = \begin{bmatrix} 1 & 0 & 0 & -\frac{1}{\rho}\partial_x & 0 \\ 0 & 1 & 0 & -\frac{1}{\rho}\partial_y & 0 \\ 0 & 0 & 1 & -\frac{1}{\rho}\partial_z & 0 \\ 0 & 0 & 0 & Q & 0 \\ 0 & 0 & 0 & 0 & 1 \end{bmatrix}, \tag{3.1}$$

so that the resulting matrix $\mathbf{L}\,\mathbf{M}$ becomes lower triangular, as

$$\mathbf{L}\,\mathbf{M} = \begin{bmatrix} Q & 0 & 0 & 0 & 0 \\ 0 & Q & 0 & 0 & 0 \\ 0 & 0 & Q & 0 & 0 \\ \rho c^2\partial_x & \rho c^2\partial_y & \rho c^2\partial_z & Q^2 - c^2\triangle & 0 \\ \frac{c^2}{\gamma}\partial_x & \frac{c^2}{\gamma}\partial_y & \frac{c^2}{\gamma}\partial_z & -\frac{c^2}{\gamma\rho}\Delta & Q \end{bmatrix}, \tag{3.2}$$

and

$$\mathbf{L}\,\mathbf{M}\,\delta\mathbf{w} \;=\; -\mathbf{R}(\mathbf{q}). \tag{3.3}$$

The main diagonal of $\mathbf{L}\,\mathbf{M}$ is composed of the factors of the matrix $\mathbf{L}$ determinant. The distributed relaxation approach yields fast convergence if the constituent scalar diagonal operators in $\mathbf{L}\,\mathbf{M}$ are solved with efficient methods.

An efficient solver for the convection factor, $Q$, can be based on downstream marching, with additional special procedures for recirculating flows [11, 12, 16, 28]. The full-potential factor, $Q^2 - c^2\triangle$, is an operator of variable type, and its solution requires different procedures in subsonic, transonic, and supersonic regions. In subsonic regions, the full-potential operator is uniformly elliptic; therefore standard multigrid methods yield optimal efficiency. When the Mach number approaches unity, the operator becomes increasingly anisotropic and, because some smooth error components cannot be approximated adequately on coarse grids, classical multigrid methods severely degrade. In supersonic regions, the full-potential operator is uniformly hyperbolic with the stream direction serving as the time-like direction. In this region, an efficient solver can be obtained with a downstream marching method. However, downstream marching becomes problematic when the Mach number drops towards unity, because marching steps allowed by the stability condition are too short. Thus, a special procedure is required to provide an efficient solution for transonic regions. A possible procedure [7, 8, 14] is based on piecewise semicoarsening and some rules for adding dissipation at the coarse grid levels.

**4. Discrete Equations.** Having in mind the distributed relaxation procedure outlined in the previous Section 3, one would like to design a discretization for nonlinear operator $\mathbf{R}(\mathbf{q})$ of (2.1) that has the discrete principal linearization operator, $\mathbf{L_h}$, satisfying properties (1) and (2) listed in Section 1. For nonconservative

formulations, the discretization of the nonlinear operator directly follows $\mathbf{L_h}$. Derivation of conservative discretization schemes corresponding to a given discrete principal-linearization operator has been discussed in [15].

In this section, we consider two factorizable discretizations for the matrix operator $\mathbf{L}$ of (2.5): the basic discretization , $\mathbf{L}^{\mathrm{h}}_{\mathrm{basic}}$, and an improved discretization, $\mathbf{L_h}$. The basic collocated-grid discretization $\mathbf{L}^{\mathrm{h}}_{\mathrm{basic}}$ of the matrix operator $\mathbf{L}$ is defined as

$$\mathbf{L}^{\mathrm{h}}_{\mathrm{basic}} = \begin{bmatrix} Q^h & 0 & 0 & \frac{1}{\rho}\partial^h_x & 0 \\ 0 & Q^h & 0 & \frac{1}{\rho}\partial^h_y & 0 \\ 0 & 0 & Q^h & \frac{1}{\rho}\partial^h_z & 0 \\ \rho c^2\partial^h_x & \rho c^2\partial^h_y & \rho c^2\partial^h_z & \bar{Q}^h & 0 \\ \frac{c^2}{\gamma}\partial^h_x & \frac{c^2}{\gamma}\partial^h_y & \frac{c^2}{\gamma}\partial^h_z & 0 & Q^h \end{bmatrix}, \tag{4.1}$$

where the discrete derivatives, $\partial^h_x, \partial^h_y, \partial^h_z$, in all off-diagonal positions are the second-order accurate central-differencing approximation. All the diagonal terms, $Q^h$, except $\bar{Q}^h$ in the fourth equation, are discretized with the same second-order accurate upwind (or upwind-biased) discretization scheme. In the subsonic regime ($|\bar{\mathbf{u}}|^2 = \bar{u}^2 + \bar{v}^2 + \bar{w}^2 < c^2$), the term $\bar{Q}^h$ is discretized with a second-order accurate downwind (or downwind-biased) discretization.

The determinant of the matrix operator $\mathbf{L}^{\mathrm{h}}_{\mathrm{basic}}$ is given by

$$\left(Q^h\right)^3 \left[Q^h\bar{Q}^h - c^2\triangle^{2h}\right], \tag{4.2}$$

where $\triangle^{2h}$ is a wide (with mesh spacing $2h$) discretization of the Laplace operator. The full-potential operator approximation appearing in the brackets has two major drawbacks:

(1) The approximation is not $h$-elliptic, i.e., it admits spurious oscillatory solutions for the discrete homogeneous equation.

(2) For near-sonic regimes (Mach number $M = |\bar{\mathbf{u}}|/c \approx 1$), the discrete operator stencil does not reflect the physical anisotropies of the differential full-potential operator. The discrete operator exhibits very strong coupling in the streamwise direction, while the differential operator has strong coupling only in the cross-stream directions.

An improved discrete full-potential operator can be obtained if the discretization $\bar{Q}^h$ is changed to $\bar{Q}^h + \mathcal{A}^h$. Then the discrete full-potential operator in (4.2) becomes

$$\mathcal{F}^h = Q^h\mathcal{A}^h + Q^h\bar{Q}^h - c^2\triangle^{2h}. \tag{4.3}$$

If the operator $\mathcal{A}^h$ is second-order small (proportional to $h^2$), the overall second-order discretization accuracy is not compromised. The choice of $\mathcal{A}^h$ used here is $\mathcal{A}^h = \left(Q^h\right)^{-1}\mathcal{D}^h, \mathcal{D}^h = \mathcal{F}^h - (Q^h\bar{Q}^h - c^2\triangle^{2h})$, where $\mathcal{F}^h$ is a desired approximation for the full-potential factor. We do not discuss in this paper the optimal discretization for the multidimensional subsonic full-potential operator. Note only that it is possible to construct a discretization that satisfies the following properties:

(1) For subsonic Mach numbers, the discretization is $h$-elliptic; in the limit of the zero Mach number, it is dominated by the narrow (with mesh spacing $h$) $h$-elliptic Laplace operator.

(2) For the Mach number approaching unity, the discretization correctly reflects the physical anisotropies and tends to the optimal discretization for the sonic-flow full-potential operator (see [7, 8, 14]).

(3) For supersonic Mach numbers, the discretization becomes upwind (or upwind-biased) and can be solved by marching.

The operator $\mathcal{A}^h$ is a nonlocal operator acting on $p^h$ and can be introduced through a new auxiliary variable $\psi^h = \mathcal{A}^h p^h$ and a new discrete equation $Q^h \psi^h = \mathcal{D}^h p^h$. Thus, the new vector of discrete unknowns becomes $\mathbf{q^h} = (u^h, v^h, w^h, \psi^h, p^h, \epsilon^h)^T$. The discrete operator $\mathbf{L}^{\mathrm{h}}_{\mathrm{basic}}$ is changed to $\mathbf{L_h}$, such that

$$\mathbf{L_h} = \begin{bmatrix} Q^h & 0 & 0 & 0 & \frac{1}{\rho}\partial_x^h & 0 \\ 0 & Q^h & 0 & 0 & \frac{1}{\rho}\partial_y^h & 0 \\ 0 & 0 & Q^h & 0 & \frac{1}{\rho}\partial_z^h & 0 \\ 0 & 0 & 0 & Q^h & -\mathcal{D}^h & 0 \\ \rho c^2 \partial_x^h & \rho c^2 \partial_y^h & \rho c^2 \partial_z^h & 1 & \bar{Q}^h & 0 \\ \frac{c^2}{\gamma}\partial_x^h & \frac{c^2}{\gamma}\partial_y^h & \frac{c^2}{\gamma}\partial_z^h & 0 & 0 & Q^h \end{bmatrix}. \tag{4.4}$$

The corresponding distribution matrix, $\mathbf{M_h}$, is defined as

$$\mathbf{M_h} = \begin{bmatrix} 1 & 0 & 0 & 0 & -\frac{1}{\rho}\partial_x^h & 0 \\ 0 & 1 & 0 & 0 & -\frac{1}{\rho}\partial_y^h & 0 \\ 0 & 0 & 1 & 0 & -\frac{1}{\rho}\partial_z^h & 0 \\ 0 & 0 & 0 & 1 & \mathcal{D}^h & 0 \\ 0 & 0 & 0 & 0 & Q^h & 0 \\ 0 & 0 & 0 & 0 & 0 & 1 \end{bmatrix}, \tag{4.5}$$

so that the resulting matrix $\mathbf{L_h}\,\mathbf{M_h}$ becomes lower triangular as

$$\mathbf{L_h}\,\mathbf{M_h} = \begin{bmatrix} Q^h & 0 & 0 & 0 & 0 & 0 \\ 0 & Q^h & 0 & 0 & 0 & 0 \\ 0 & 0 & Q^h & 0 & 0 & 0 \\ 0 & 0 & 0 & Q^h & 0 & 0 \\ \rho c^2 \partial_x^h & \rho c^2 \partial_y^h & \rho c^2 \partial_z^h & 1 & \mathcal{F}^h & 0 \\ \frac{c^2}{\gamma}\partial_x^h & \frac{c^2}{\gamma}\partial_y^h & \frac{c^2}{\gamma}\partial_z^h & 0 & -\frac{c^2}{\gamma\rho}\Delta^{2h} & Q^h \end{bmatrix}. \tag{4.6}$$

**5. One-Dimensional Model Problem.** The set of the quasi-one-dimensional nonconservative Euler equations is given by

$$\begin{aligned} u\partial_x u + \tfrac{1}{\rho}\partial_x p &= 0, \\ \rho c^2 \partial_x u + u\partial_x p &= -\gamma p u \tfrac{\sigma_x}{\sigma}, \\ (\gamma-1)\epsilon\partial_x u + u\partial_x \epsilon &= -(\gamma-1)\epsilon u \tfrac{\sigma_x}{\sigma}, \end{aligned} \tag{5.1}$$

where $\sigma(x)$ is the area distribution. The principal linearization of the operator in (5.1), in the limit as $h$ tends to zero, is

$$\begin{pmatrix} \bar{u}\partial_x & \frac{1}{\rho}\partial_x & 0 \\ \rho c^2 \partial_x & \bar{u}\partial_x & 0 \\ (\gamma-1)\bar{\epsilon}\partial_x & 0 & \bar{u}\partial_x \end{pmatrix}, \tag{5.2}$$

in which the coefficients $\bar{u}, \rho, c$, and $\bar{\epsilon}$ are constants unrelated to the unknown functions $(u, p, \epsilon)$. The third equation is decoupled from the other equations. Thus, for the purpose of analysis, one can focus on the system of two constant-coefficient equations

$$\mathbf{L}\ \mathbf{q} = \mathbf{f}, \tag{5.3}$$

where

$$\mathbf{L} = \begin{pmatrix} \bar{u}\partial_x & \frac{1}{\rho}\partial_x \\ \rho c^2 \partial_x & \bar{u}\partial_x \end{pmatrix}, \tag{5.4}$$

$\mathbf{f} = (f_1, f_2)^T$, and $\mathbf{q} = (u, p)^T$. For the subsonic flow regimes, a natural set of boundary conditions for this model problem is $u$ specified at the inflow boundary and $p$ specified at the outflow boundary. With this set of boundary conditions, the differential problem (5.3) is well posed.

The analysis presented in this section compares the exact differential and discrete solutions for $u$ and $p$ obtained for the model problem (5.3). Let the exact solution of (5.3) defined on the interval $x \in [0, 1]$ be

$$\mathbf{q}_{\text{exact}}(x) = \begin{pmatrix} u_{\text{exact}} \\ p_{\text{exact}} \end{pmatrix} = \begin{pmatrix} C_u \\ C_p \end{pmatrix} e^{i\alpha x}, \tag{5.5}$$

where $\alpha$ is an arbitrary frequency. Then

$$\begin{pmatrix} f_1(x) \\ f_2(x) \end{pmatrix} = \begin{pmatrix} \bar{f}_1 \\ \bar{f}_2 \end{pmatrix} e^{i\alpha x}, \qquad \begin{pmatrix} \bar{f}_1 \\ \bar{f}_2 \end{pmatrix} = \begin{pmatrix} \bar{u}C_u + \frac{1}{\rho}C_p \\ \rho c^2 C_u + \bar{u}C_p \end{pmatrix} i\alpha. \tag{5.6}$$

The system (5.3) is subject to boundary conditions

$$u(0) = C_u, \qquad p(1) = C_p e^{i\alpha}. \tag{5.7}$$

The distribution matrix $\mathbf{M}$,

$$\mathbf{M} = \begin{pmatrix} 1 & -\frac{1}{\rho}\partial_x \\ 0 & \bar{u}\partial_x \end{pmatrix}, \tag{5.8}$$

results in

$$\mathbf{LM} = \begin{pmatrix} \bar{u}\partial_x & 0 \\ \rho c^2 \partial_x & \mathcal{F} \end{pmatrix}. \tag{5.9}$$

The main diagonal of matrix $\mathbf{LM}$ is composed of the convection operator $\bar{u}\partial_x$ and the full-potential operator $\mathcal{F} = (\bar{u}^2 - c^2)\partial_{xx}$. The one-dimensional problem is very specific for at least two reasons:

(1) The full-potential factor vanishes at the sonic speed ($\bar{u} = c$).

(2) The characteristics perfectly align with the grid.

Both these features disappear in multiple dimensions.

The corresponding discrete problem is defined on a uniform grid with mesh size $h$ as

$$\mathbf{L_h}\ \mathbf{q^h} = \mathbf{f^h}, \tag{5.10}$$

where $\mathbf{L_h}$ is a discretization of $\mathbf{L}$, and $\mathbf{q}_j^{\mathbf{h}} = (u_j^h, p_j^h)^T$ and $\mathbf{f}_j^{\mathbf{h}} = (f_1(jh), f_2(jh))^T$ are discrete representations of the solutions and source functions, respectively, and $j = 0, 1, 2, \ldots, N$, $N = 1/h$. The general solution to (5.10) can be sought as a combination of a particular solution and the general solution to the corresponding homogeneous problem

$$\mathbf{L_h}\ \mathbf{q^h} = 0. \tag{5.11}$$

A particular solution can be found in the form

$$\mathbf{q}_{\text{par}}^{\mathbf{h}} = \begin{pmatrix} u_{\text{par}}^h \\ p_{\text{par}}^h \end{pmatrix}_j = \begin{pmatrix} \hat{u} \\ \hat{p} \end{pmatrix} e^{i\omega j}, \tag{5.12}$$

$$\begin{pmatrix} \hat{u} \\ \hat{p} \end{pmatrix} = \left(\mathbf{L_h}(e^{i\omega})\right)^{-1} \begin{pmatrix} \bar{f}_1 \\ \bar{f}_2 \end{pmatrix}, \tag{5.13}$$

where $\omega = \alpha h$ is a normalized frequency, and $\mathbf{L_h}(\lambda)$ is a generalized matrix symbol of the discrete operator $\mathbf{L_h}$. The entries of $\mathbf{L_h}(\lambda)$ are generalized symbols of the discrete scalar operators composing $\mathbf{L_h}$ that are defined as responses of these operators on the exponent function $\lambda^j$. For example, the generalized symbol, $\partial^c(\lambda)$, of the central second-order accurate difference approximation to the first derivative, $\partial^c$, is $\partial^c \lambda^j = \partial^c(\lambda)\lambda^j$, $\partial^c(\lambda) = \frac{1}{2h}\left(\lambda - \frac{1}{\lambda}\right)$.

The general solution, $\mathbf{q}^{\mathbf{h}}_{\text{hom}}$, of the homogeneous system of equations (5.11) is a combination of linearly independent characteristic solutions $\mathbf{z}_k = \mathbf{v}_k \lambda_k^j$, where $\lambda_k$ are the roots of the characteristic polynomial

$$\det \mathbf{L_h}(\lambda) = 0. \tag{5.14}$$

$$\mathbf{q}^{\mathbf{h}}_{\text{hom}} = \begin{pmatrix} u^h_{\text{hom}} \\ p^h_{\text{hom}} \end{pmatrix}_j = \sum_k c_k \mathbf{z}_k(j) = \sum_k c_k \mathbf{v}_k \lambda_k^j. \tag{5.15}$$

The general solution of the discrete problem (5.10) is

$$\mathbf{q}^{\mathbf{h}} = \mathbf{q}^{\mathbf{h}}_{\text{hom}} + \mathbf{q}^{\mathbf{h}}_{\text{par}} = \sum_k c_k \mathbf{z}_k(j) + \begin{pmatrix} \hat{u} \\ \hat{p} \end{pmatrix} e^{i\omega j}. \tag{5.16}$$

Parameters $c_k$ are chosen to satisfy a set of discrete boundary conditions. The discretization error function is defined as

$$\mathbf{q}^h - \mathbf{q}^h_{\text{exact}}, \tag{5.17}$$

where $\mathbf{q}^h_{\text{exact}}$ is a restriction of $\mathbf{q}_{\text{exact}}(x)$ to the grid with the mesh size $h$.

Below, the discretization errors for four discrete factorizable schemes approximating (5.3) are compared:

*Scheme # 1.* The "basic" scheme of the (4.1) type.

*Scheme # 2.* The standard upwind discrete scheme.

*Scheme # 3.* The discrete scheme of the (4.4) type with the discretization for the full-potential factor given as

$$\mathcal{F}^h = \left(\bar{u}^2 - c^2\right)\partial^u \partial^d, \tag{5.18}$$

where the discrete operators, $\partial^u$ and $\partial^d$, are second-order accurate upwind and downwind difference approximations to the first derivative, respectively.

(4) *Scheme # 4.* The discrete scheme of the (4.4) type with the discretization for the full-potential factor given as

$$\mathcal{F}^h = \left(\bar{u}^2 - c^2\right)\partial^h_{xx}, \tag{5.19}$$

where the discrete operator $\partial^h_{xx}$ is a three-point central approximation to the second derivative.

All the schemes, except the standard upwind scheme (2), are factorizable in multiple dimensions. The discrete boundary conditions for all the four schemes are overspecified, i.e., the discrete-solution values at the boundary and, wherever necessary, outside of the target computational domain are specified from the known exact solution (5.5).

**5.1. Scheme # 1.** The one-dimensional version of the "basic" collocated-grid discretization for matrix operator $\mathbf{L}$ of (5.3) is defined as

$$\mathbf{L}_{\mathbf{h}}^{(\mathbf{1})}\ \mathbf{q}^{(\mathbf{1})} = \mathbf{f}^{\mathbf{h}}, \tag{5.20}$$

$$\mathbf{L}_{\mathbf{h}}^{(\mathbf{1})} = \begin{bmatrix} \bar{u}\partial^u & \frac{1}{\rho}\partial^c \\ \rho c^2 \partial^c & \bar{u}\partial^d \end{bmatrix}. \tag{5.21}$$

Recall that the discrete derivatives, $\partial^u, \partial^c$, and $\partial^d$, are second-order accurate upwind, central, and downwind difference approximations, respectively.

The generalized symbol for the operator $\mathbf{L}_{\mathbf{h}}^{(\mathbf{1})}$ is defined as

$$\mathbf{L}_{\mathbf{h}}^{(\mathbf{1})}(\lambda) = \begin{pmatrix} \bar{u}\partial^u(\lambda) & \frac{1}{\rho}\partial^c(\lambda) \\ \rho c^2 \partial^c(\lambda) & \bar{u}\partial^d(\lambda) \end{pmatrix}, \tag{5.22}$$

where

$$\begin{aligned} \partial^u(\lambda) &= \tfrac{1}{h}\left(\tfrac{3}{2} - 2\tfrac{1}{\lambda} + \tfrac{1}{2}\tfrac{1}{\lambda^2}\right), \\ \partial^d(\lambda) &= \tfrac{1}{h}\left(-\tfrac{3}{2} + 2\lambda - \tfrac{1}{2}\lambda^2\right), \\ \partial^c(\lambda) &= \tfrac{1}{h}\left(\tfrac{1}{2}\lambda - \tfrac{1}{2}\tfrac{1}{\lambda}\right). \end{aligned} \tag{5.23}$$

A particular solution to (5.20) is

$$\mathbf{q}_{\mathrm{par}}^{(\mathbf{1})} = \begin{pmatrix} \hat{u}^{(1)} \\ \hat{p}^{(1)} \end{pmatrix} e^{i\omega j}, \tag{5.24}$$

where

$$\begin{aligned} \hat{u}^{(1)} &= \frac{\bar{u}\partial^d(e^{i\omega})\bar{f}_1 - \frac{1}{\rho}\partial^c(e^{i\omega})\bar{f}_2}{\bar{u}^2\partial^u(e^{i\omega})\partial^d(e^{i\omega}) - c^2(\partial^c(e^{i\omega}))^2}, \\ \hat{p}^{(1)} &= \frac{-\rho c^2\partial^c(e^{i\omega})\bar{f}_1 + \bar{u}\partial^u(e^{i\omega})\bar{f}_2}{\bar{u}^2\partial^u(e^{i\omega})\partial^d(e^{i\omega}) - c^2(\partial^c(e^{i\omega}))^2}. \end{aligned} \tag{5.25}$$

A set of linearly independent characteristic solutions $\mathbf{z}_k(j) = \mathbf{v}_k\lambda_k^j$ is given by

$$\mathbf{v}_1 = \begin{pmatrix} 1 \\ 0 \end{pmatrix} \ \text{ and } \ \mathbf{v}_2 = \begin{pmatrix} 0 \\ 1 \end{pmatrix}, \tag{5.26}$$

which corresponds to $\lambda_{1,2} = 1$;

$$\mathbf{v}_3 = \begin{pmatrix} 1 \\ -\frac{\rho\bar{u}\partial^u(\lambda_3)}{\partial^c(\lambda_3)} \end{pmatrix}, \tag{5.27}$$

which corresponds to $\lambda_3 = \frac{5\bar{u}^2 - c^2 - 4\bar{u}\sqrt{\bar{u}^2 - c^2}}{3\bar{u}^2 + c^2}$; and

$$\mathbf{v}_4 = \begin{pmatrix} 1 \\ -\frac{\rho\bar{u}\partial^u(\lambda_4)}{\partial^c(\lambda_4)} \end{pmatrix} \tag{5.28}$$

which corresponds to $\lambda_4 = \frac{5\bar{u}^2 - c^2 + 4\bar{u}\sqrt{\bar{u}^2 - c^2}}{3\bar{u}^2 + c^2}$.

The characteristic solutions $\mathbf{z}_k$ are normalized to satisfy $\max_j |\mathbf{z}_k(j)| = O(1)$ as $h$ tends to zero. The characteristic solutions $\mathbf{z}_1$ and $\mathbf{z}_2$ correspond to solutions of the target differential problem; the characteristic

solutions $\mathbf{z}_3$ and $\mathbf{z}_4$ are numerical artifacts. Note that in subsonic regimes, $|\lambda_3| = |\lambda_4| = 1$; this implies existence of global discrete solutions that do not approximate solutions of the differential problem. These spurious solutions are a source of instability of the discrete approximation (5.20). Details are given in Appendix A. For stable approximations, characteristic solutions unrelated to the differential solutions should be local, i.e., they should correspond to $|\lambda_k| \neq 1$. The coefficients $c_k$ are computed from a 4×4 linear system that arises after substituting the general solution into the boundary condition equations

$$
\begin{array}{lll}
\text{(i)} & u_0^h & = C_u, \\
\text{(ii)} & \frac{\bar{u}}{h}\Big(\frac{3}{2}u_1^h - 2u_0^h + \frac{1}{2}u_{-1}^h\Big) + \frac{1}{\rho h}\Big(\frac{1}{2}p_2^h - \frac{1}{2}p_0^h\Big) & = f_1(h), \\
\text{(iii)} & \frac{\rho c^2}{h}\Big(\frac{1}{2}u_N^h - \frac{1}{2}u_{N-2}^h\Big) + \frac{\bar{u}}{h}\Big(-\frac{3}{2}p_{N-1}^h + 2p_N^h - \frac{1}{2}p_{N+1}^h\Big) & = f_2(1-h), \\
\text{(iv)} & p_N^h & = C_p e^{i\alpha},
\end{array}
\tag{5.29}
$$

where values $u_{-1}^h, p_0^h, u_N^h$, and $p_{N+1}^h$ are specified from the exact solution (5.5).

**5.2. Scheme # 2.** A one-dimensional version of the standard upwind scheme for matrix operator $\mathbf{L}$ of (5.3) is defined as

$$
\mathbf{L}_{\mathbf{h}}^{(\mathbf{2})}\mathbf{q}^{(\mathbf{2})} = \mathbf{f}^{\mathbf{h}},
\tag{5.30}
$$

$$
\mathbf{L}_{\mathbf{h}}^{(\mathbf{2})} = \begin{bmatrix} \frac{\bar{u}+c}{2}\partial^u + \frac{\bar{u}-c}{2}\partial^d & \frac{\bar{u}+c}{2\rho c}\partial^u - \frac{\bar{u}-c}{2\rho c}\partial^d \\ \frac{\rho c(\bar{u}+c)}{2}\partial^u - \frac{\rho c(\bar{u}-c)}{2}\partial^d & \frac{\bar{u}+c}{2}\partial^u + \frac{\bar{u}-c}{2}\partial^d \end{bmatrix}.
\tag{5.31}
$$

The following four boundary conditions (two from the left and two from the right) are used by the interior discretizations:

$$
\begin{array}{lll}
\text{(i)} & \frac{1}{2}u_0^h + \frac{1}{2\rho c}p_0^h & = \frac{1}{2}C_u + \frac{1}{2\rho c}C_p, \\
\text{(ii)} & \frac{1}{2}u_{-1}^h + \frac{1}{2\rho c}p_{-1}^h & = \Big(\frac{1}{2}C_u + \frac{1}{2\rho c}C_p\Big)e^{-i\omega}, \\
\text{(iii)} & \frac{1}{2}u_{N+1}^h - \frac{1}{2\rho c}p_{N+1}^h & = \Big(\frac{1}{2}C_u - \frac{1}{2\rho c}C_p\Big)e^{i\omega(N+1)}, \\
\text{(iv)} & \frac{1}{2}u_N^h - \frac{1}{2\rho c}p_N^h & = \Big(\frac{1}{2}C_u - \frac{1}{2\rho c}C_p\Big)e^{i\omega N}.
\end{array}
\tag{5.32}
$$

A particular solution can be found in the form

$$
\mathbf{q}_{\text{par}}^{(\mathbf{2})} = \begin{pmatrix} \hat{u}^{(2)} \\ \hat{p}^{(2)} \end{pmatrix} e^{i\omega j},
\tag{5.33}
$$

where

$$
\begin{aligned}
\hat{u}^{(2)} &= \frac{\big(\frac{\bar{u}+c}{2}\partial^u(e^{i\omega}) + \frac{\bar{u}-c}{2}\partial^d(e^{i\omega})\big)\bar{f}_1 - \frac{1}{\rho c}\big(\frac{\bar{u}+c}{2}\partial^u(e^{i\omega}) - \frac{\bar{u}-c}{2}\partial^d(e^{i\omega})\big)\bar{f}_2}{(\bar{u}^2-c^2)\partial^u(e^{i\omega})\partial^d(e^{i\omega})}, \\
\hat{p}^{(2)} &= \frac{-\rho c\big(\frac{\bar{u}+c}{2}\partial^u(e^{i\omega}) - \frac{\bar{u}-c}{2}\partial^d(e^{i\omega})\big)\bar{f}_1 + \big(\frac{\bar{u}+c}{2}\partial^u(e^{i\omega}) + \frac{\bar{u}-c}{2}\partial^d(e^{i\omega})\big)\bar{f}_2}{(\bar{u}^2-c^2)\partial^u(e^{i\omega})\partial^d(e^{i\omega})}.
\end{aligned}
\tag{5.34}
$$

A set of linearly independent characteristic solutions $\mathbf{z}_k(j) = \mathbf{v}_k\lambda_k^j$ is given by

$$
\mathbf{v}_1 = \begin{pmatrix} 1 \\ 0 \end{pmatrix} \text{ and } \mathbf{v}_2 = \begin{pmatrix} 0 \\ 1 \end{pmatrix},
\tag{5.35}
$$

which corresponds to $\lambda_{1,2} = 1$;

$$
\mathbf{v}_3 = \begin{pmatrix} 1 \\ \rho c \end{pmatrix},
\tag{5.36}
$$

which corresponds to $\lambda_3 = \frac{1}{3}$; and

$$\mathbf{v}_4 = (\lambda_4)^{-N} \begin{pmatrix} 1 \\ -\rho c \end{pmatrix} \tag{5.37}$$

which corresponds to $\lambda_4 = 3$. The characteristic solutions $\mathbf{z}_1$ and $\mathbf{z}_2$ approximate solutions of the differential equations; the characteristic solutions $\mathbf{z}_3$ and $\mathbf{z}_4$ are local. The discrete scheme (5.30) is stable. The coefficients $c_k$ are found by substituting the general solution into (5.32).

**5.3. Scheme # 3.** A factorizable scheme corresponding to (4.4) is defined as

$$\mathbf{L}_{\mathbf{h}}^{(\mathbf{3})} \mathbf{q}^{(\mathbf{3})} = \mathbf{f}^{\mathbf{h}}, \tag{5.38}$$

$$\mathbf{L}_{\mathbf{h}}^{(\mathbf{3})} = \begin{pmatrix} \bar{u}\partial^u & 0 & \frac{1}{\rho}\partial^c \\ 0 & \bar{u}\partial^u & -\mathcal{D}^h \\ \rho c^2 \partial^c & 1 & \bar{u}\partial^d \end{pmatrix}, \qquad \mathbf{q}^{(\mathbf{3})} = \begin{pmatrix} u^h \\ \psi^h \\ p^h \end{pmatrix}, \qquad \mathbf{f}^{\mathbf{h}} = \begin{pmatrix} f_1(jh) \\ 0 \\ f_2(jh) \end{pmatrix}, \tag{5.39}$$

$$\mathcal{D}^h = \mathcal{F}^h - \left( \bar{u}^2 \partial^u \partial^d - c^2 \left(\partial^c\right)^2 \right), \tag{5.40}$$

and the desired discrete full-potential operator is given by

$$\mathcal{F}^h = (\bar{u}^2 - c^2) \partial^u \partial^d. \tag{5.41}$$

The overspecified boundary conditions, where values of $u_{-1}^h, u_0^h, u_N^h, u_{N+1}^h, p_{-1}^h, p_0^h, p_N^h$, and $p_{N+1}^h$ are specified from the exact differential solution (5.5), and $\psi_{-1}^h = \psi_0^h = \psi_N^h = \psi_{N+1}^h = 0$, are equivalent to the following six boundary conditions:

$$\begin{array}{lll} \text{(i)} & u_0^h & = C_u, \\ \text{(ii)} & \bar{u}\partial^u u_1^h + \frac{1}{\rho}\partial^c p_1^h & = f_1(h), \\ \text{(iii)} & \bar{u}\partial^u \psi_1^h - \mathcal{D}^h p_1^h & = 0, \\ \text{(iv)} & \bar{u}\partial^u \psi_2^h - \mathcal{D}^h p_2^h & = 0, \\ \text{(v)} & \rho c^2 \partial^c u_{N-1}^h + \psi_{N-1}^h + \bar{u}\partial^d p_{N-1}^h & = f_2(1-h), \\ \text{(vi)} & p_N^h & = C_p e^{i\alpha}. \end{array} \tag{5.42}$$

In evaluation of (v), the value of $\psi_{N-1}^h$ is computed from the equation $\bar{u}\partial^u \psi_{N-1}^h - \mathcal{D}^h p_{N-1}^h = 0$.

A particular solution of the nonhomogeneous problem can be found as

$$\mathbf{q}_{\text{par}}^{(\mathbf{3})} = \begin{pmatrix} \hat{u}^{(3)} \\ \hat{\psi}^{(3)} \\ \hat{p}^{(3)} \end{pmatrix} e^{i\omega j}, \tag{5.43}$$

where

$$\begin{aligned} \hat{u}^{(3)} &= \frac{1}{\bar{u}\partial^u(e^{i\omega})} \left( \bar{f}_1 - \frac{\partial^c(e^{i\omega})}{\rho} \left( \frac{-\rho c^2 \partial^c(e^{i\omega}) \bar{f}_1 + \bar{u}\partial^u(e^{i\omega}) \bar{f}_2}{\mathcal{F}^h(e^{i\omega})} \right) \right), \\ \hat{\psi}^{(3)} &= \frac{\mathcal{D}^h(e^{i\omega})}{\bar{u}\partial^u(e^{i\omega})} \left( \frac{-\rho c^2 \partial^c(e^{i\omega}) \bar{f}_1 + \bar{u}\partial^u(e^{i\omega}) \bar{f}_2}{\mathcal{F}^h(e^{i\omega})} \right), \\ \hat{p}^{(3)} &= \frac{-\rho c^2 \partial^c(e^{i\omega}) \bar{f}_1 + \bar{u}\partial^u(e^{i\omega}) \bar{f}_2}{\mathcal{F}^h(e^{i\omega})}. \end{aligned} \tag{5.44}$$

The generalized symbols $\partial^u(\lambda), \partial^c(\lambda)$, and $\partial^d(\lambda)$ are defined in (5.23) and

$$\begin{aligned} \mathcal{F}^h(\lambda) = &\quad (\bar{u}^2 - c^2)\partial^u(\lambda)\partial^d(\lambda), \\ \mathcal{D}^h(\lambda) = &\quad c^2\Big((\partial^c(\lambda))^2 - \partial^u(\lambda)\partial^d(\lambda)\Big) = \tfrac{c^2}{h^2}\Big(\tfrac{1}{\lambda^2} - 4\tfrac{1}{\lambda} + 6 - 4\lambda + \lambda^2\Big). \end{aligned} \tag{5.45}$$

The six linearly independent characteristic solutions, $\mathbf{z}_k(j) = \mathbf{v}_k(j)\lambda_k^j$, are given by

$$\mathbf{v}_1 = \begin{pmatrix} 1 \\ 0 \\ 0 \end{pmatrix}, \mathbf{v}_2 = \begin{pmatrix} 0 \\ 0 \\ 1 \end{pmatrix}, \text{ and } \mathbf{v}_3 = \begin{pmatrix} jh \\ \rho c^2\left(\frac{\bar{u}^2}{c^2} - 1\right) \\ -jh\rho\bar{u} \end{pmatrix} \tag{5.46}$$

which corresponds to $\lambda_{1,2,3} = 1$,

$$\mathbf{v}_4 = \begin{pmatrix} h \\ -\rho c^2 h\partial^c(\lambda_4) \\ 0 \end{pmatrix} = \begin{pmatrix} h \\ \frac{4}{3}\rho c^2 \\ 0 \end{pmatrix}$$

and (5.47)

$$\mathbf{v}_5 = \begin{pmatrix} jh \\ \rho c^2 h\left(\frac{\bar{u}^2}{c^2}\frac{\partial^d(\lambda_5)\hat{\partial^u}(\lambda_5)}{\partial^c(\lambda_5)} - \hat{\partial^c}(\lambda_5) - j\partial^c(\lambda_5)\right) \\ -h\rho\bar{u}\frac{\hat{\partial^u}(\lambda_5)}{\partial^c(\lambda_5)} \end{pmatrix} = \begin{pmatrix} jh \\ \rho c^2\left(-2\frac{\bar{u}^2}{c^2} - \frac{5}{3} + j\frac{4}{3}\right) \\ -\frac{9}{4}h\rho\bar{u} \end{pmatrix},$$

which corresponds to $\lambda_{4,5} = \frac{1}{3}$, where $\hat{\partial^u}(\lambda) = \frac{1}{h}\left(2\frac{1}{\lambda} - \frac{1}{\lambda^2}\right)$ and $\hat{\partial^c}(\lambda) = \frac{1}{h}\left(\frac{1}{2}\frac{1}{\lambda} + \frac{1}{2}\lambda\right)$;

and

$$\mathbf{v}_6 = (\lambda_6)^{-N}\begin{pmatrix} h \\ -\rho c^2 h\partial^c(\lambda_6) \\ -h\rho\bar{u}\frac{\partial^u(\lambda_6)}{\partial^c(\lambda_6)} \end{pmatrix} = (\lambda_6)^{-N}\begin{pmatrix} h \\ -\frac{4}{3}\rho c^2 \\ -h\frac{2}{3}\rho\bar{u} \end{pmatrix}, \tag{5.48}$$

which corresponds to $\lambda_6 = 3$. The characteristic solutions are normalized to satisfy $\max_j |\mathbf{z}_k(j)| = O(1)$ for $h$ tending to zero.

**5.4. Scheme # 4.** Another factorizable scheme belonging to the family (4.4) is defined as

$$\mathbf{L}_{\mathbf{h}}^{(\mathbf{4})}\mathbf{q}^{(\mathbf{4})} = \mathbf{f}^{\mathbf{h}}, \tag{5.49}$$

where $\mathbf{L}_{\mathbf{h}}^{(\mathbf{4})}$ is similar to $\mathbf{L}_{\mathbf{h}}^{(\mathbf{3})}$ with the desired discretization for the full-potential factor given as

$$\mathcal{F}^h = (\bar{u}^2 - c^2)\partial_{xx}^h, \tag{5.50}$$

where $\partial_{xx}^h$ is a three-point central second-order accurate approximation to the second derivative. The vector-function $\mathbf{q}^{(\mathbf{4})}$ is defined similar to $\mathbf{q}^{(\mathbf{3})}$.

A particular solution can be found in the form of (5.43) and (5.44) with the generalized symbols

$$\begin{aligned} \mathcal{F}^h(\lambda) = &\quad (\bar{u}^2 - c^2)\partial_{xx}^h(\lambda) = \tfrac{\bar{u}^2 - c^2}{h^2}\Big(\tfrac{1}{\lambda} - 2 + \lambda\Big), \\ \mathcal{D}^h(\lambda) = &\quad \mathcal{F}^h(\lambda) - \left(\bar{u}^2\partial^u(\lambda)\partial^d(\lambda) - c^2(\partial^c(\lambda))^2\right). \end{aligned} \tag{5.51}$$

The "maximal-length footprint" stencil of the $\mathbf{L}_{\mathbf{h}}^{(\mathbf{4})}$ determinant operator computed before any cancellation occur includes seven points. Based on this stencil, the corresponding characteristic equation is formed as

$$\frac{\bar{u}(\bar{u}^2 - c^2)}{2h}\left(0\frac{1}{\lambda^4} + \frac{1}{\lambda^3} - 6\frac{1}{\lambda^2} + 12\frac{1}{\lambda} - 10 + 3\lambda + 0\lambda^2\right) = 0. \tag{5.52}$$

For the characteristic equation, zero coefficients in the leftmost positions imply zero roots, and, in the rightmost positions, they imply infinite roots. Six roots of equation (5.52) are $\lambda_{1,2,3} = 1$, $\lambda_4 = \frac{1}{3}$, $\lambda_5 = 0$, and $\lambda_6 = \infty$.

The solution representation as a linear combination of the functions $\mathbf{z}_k = \mathbf{v}_k \lambda_k^j$ is relevant only for finite $\lambda_k \neq 0$. For $\lambda_k = 0$, the corresponding characteristic solutions are localized at the inflow boundary, i.e., they exhibit nonzero values at the inflow and are zero in the interior and at the outflow boundary. By analogy, characteristic solutions which corresponds to $\lambda_k = \infty$ are localized at the outflow boundary, i.e., they are nonzero only at some locations in the vicinity of the outflow boundary.

Four linearly independent characteristic solutions which corresponds to finite (nonzero) $\lambda_k$ can be found in the usual form $\mathbf{z}_k(j) = \mathbf{v}_k \lambda_k^j$.

$$\mathbf{v}_1 = \begin{pmatrix} 1 \\ 0 \\ 0 \end{pmatrix}, \mathbf{v}_2 = \begin{pmatrix} 0 \\ 0 \\ 1 \end{pmatrix}, \text{ and } \mathbf{v}_3 = \begin{pmatrix} jh \\ \rho\left(\bar{u}^2 - c^2\right) \\ -jh\rho\bar{u} \end{pmatrix} \tag{5.53}$$

correspond to $\lambda_{1,2,3} = 1$, and

$$\mathbf{v}_4 = \begin{pmatrix} h \\ -h\rho c^2 \partial^c(\lambda_4) \\ 0 \end{pmatrix} = \begin{pmatrix} h \\ \frac{4}{3}\rho c^2 \\ 0 \end{pmatrix} \tag{5.54}$$

corresponds to $\lambda_4 = \frac{1}{3}$.

The characteristic solution $\mathbf{z}_5$ localized at the inflow (i.e., corresponding to $\lambda_5 = 0$) is

$$\mathbf{z}_5(j) = \begin{pmatrix} h\,\delta_j^0 \\ \rho\frac{3\bar{u}^2+c^2}{2}\,\delta_j^1 \\ \rho\bar{u}h\,\delta_j^1 \end{pmatrix}, \tag{5.55}$$

and the characteristic solution $\mathbf{z}_6$ localized at the outflow (i.e., corresponding to $\lambda_6 = \infty$) is

$$\mathbf{z}_6(j) = \begin{pmatrix} h\,\delta_j^{N-1} \\ -\rho\frac{3\bar{u}^2+c^2}{2}\,\delta_j^{N-2} \\ -3\rho\bar{u}h\,\delta_j^N \end{pmatrix}, \tag{5.56}$$

where

$$\delta_j^m = \begin{cases} 0, & \text{if} \quad m \neq j, \\ 1, & \text{if} \quad m = j. \end{cases} \tag{5.57}$$

Coefficients $c_k, k = 1, \ldots, 6$ can be found by substituting the general solution into the boundary condition equations that are similar to (5.42) with discretization $\mathcal{D}^h$ (5.40) corresponding to $\mathcal{F}^h$ defined in (5.50).

**5.5. Discretization Errors.** In this section, the $L_\infty$ norms of discretization errors in $p$ for Schemes # 1 through # 4 are compared for the constant-coefficient problems corresponding to different Mach numbers ($M = 0.01, 0.5, 0.99$, and $M^* = \sqrt{\frac{13+8\sqrt{2}}{41}} \approx 0.88$). The value of $M^*$ has been chosen to illustrate an erratic convergence history for the Scheme # 1. More details are given in Appendix A. The constant coefficients nondimensionalized with respect to the density and the speed of sound at the sonic conditions are defined as

$$\begin{aligned} c &= \sqrt{\frac{1+\frac{\gamma-1}{2}}{1+M^2\frac{\gamma-1}{2}}}, \\ \rho &= c^{\frac{2}{\gamma-1}}, \\ \bar{u} &= cM, \end{aligned} \tag{5.58}$$

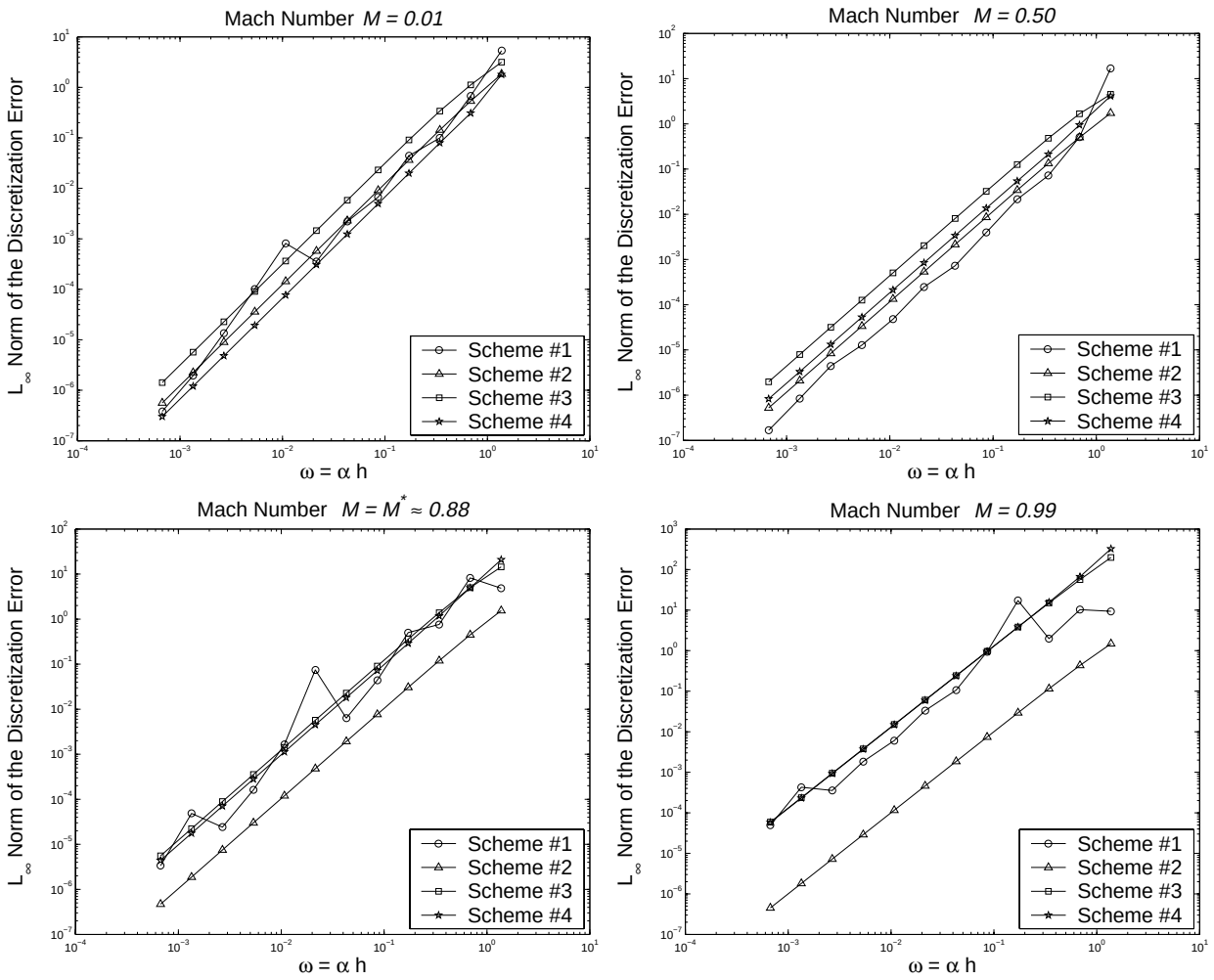


FIG. 5.1. *$L_\infty$ norms of discretization errors in pressure.*

where $\gamma = 1.4$. The parameters of the exact differential solution defined on the interval $x \in [0, 1]$ have been chosen as $C_u = 1, C_p = 2$, and $\alpha = 7\pi$. The $L_\infty$ norms of discretization errors in pressure, $p$, plotted on Figure 5.1 have been computed for solutions on a sequence of uniform grids with $h = 2^{-4}, 2^{-5}, \ldots, 2^{-15}$.

For low to medium subsonic Mach numbers, the discretization errors of the new factorizable schemes (# 3 and # 4) are very competitive with the discretization errors of standard schemes (# 1 and # 2) on all the grids. In this range of Mach numbers, the discretization errors of Scheme #4 are smaller than the discretization errors of Scheme #3. The discretization accuracy of Scheme # 3 differs from the accuracy of Scheme # 4 because of the difference in the five-point and three-point approximations to the full-potential factor. The differences vanish as the Mach number tends to unity because the contribution of the full-potential factor becomes negligible.

For subsonic Mach numbers approaching unity, the characteristic-upwinding Scheme # 2 is obviously superior, exhibiting discretization errors that are nearly two orders of magnitude smaller that the discretization errors achieved by other schemes on the same grids. Although not shown in the figures, the situation is similar for errors in velocity at Mach numbers approaching zero. Scheme # 2 in one dimension is very close to ideal because the entire system can be cast as three scalar convection equations. A standard dimension-

by-dimension extension to multiple dimensions loses this property as well as the more fundamental property of discrete factorizability. Thus, in multiple dimensions, the new factorizable schemes proposed in this paper are expected to offer comparable accuracy and considerable improvements in efficiency.

As shown in Figure 5.1, convergence of discretization errors for Scheme # 1 may be very erratic. This behavior is explained by presence of the spurious global solutions. In particular, the choice of the Mach number $M = M^*$ corresponds to the spurious solutions varying as $e^{\pm i\frac{\pi}{4}j}$. A pattern of discretization error increases on each fourth grid is notable in the test with $M = M^*$. Analysis performed in Appendix A confirms that the discretization error convergence rates for this scheme do not settle to any particular value. The mean convergence, however, obeys the order property. The convergence rate pattern is dictated by the characteristic frequency of the spurious solutions. The new factorizable schemes overcome this disorder and exhibit monotonic convergence rates with an asymptote determined by the approximation order of the discretizations in the interior.

Another interesting feature associated with the new factorizable schemes is the asymptotic behavior of the auxiliary discrete function $\psi^h$. The amplitude of this function is $O(h)$ in some $O(h)$-small neighborhoods of the boundaries and decreases exponentially quickly to $O(h^2)$-size in the interior. This behavior does not compromise the second-order accuracy in the physical variables $u^h$ and $p^h$. It is explained by interactions of the interior discretizations with the overspecified boundary conditions. The amplitude of $\psi^h$ becomes uniformly $O(h^2)$-small if another set of boundary conditions that better suit the interior discretizations is applied.

**6. Multigrid Method.** An FMG algorithm solves the target-grid equations proceeding from the coarsest grid to finer grids. The goal of the algorithm is fast reduction of the current-grid algebraic errors below the level of discretization errors, before interpolating solutions to the next finer grid. The algebraic errors on a given grid, which are defined as the differences between the approximate and exact discrete solutions, are reduced through a Full Approximation Scheme (FAS) [3, 4, 13, 22, 26, 27] multigrid cycle, in which corrections to the fine-grid nonlinear equations are obtained from coarser grid solutions. The FMG-FAS method is described below by means of a two-grid notation, in which the fine grid is denoted by superscript $h$ and the coarse grid by superscript $2h$.

Let the fine-grid nonlinear equations be defined as

$$\mathbf{R^h}(\mathbf{q}^h) = \mathbf{f}^h. \tag{6.1}$$

The initial fine-grid solution approximation $\mathbf{q}^h$ is prolonged from the coarse-grid solutions $\mathbf{q}^{2h}$, as

$$\mathbf{q}^h = \hat{\mathcal{P}}\,\mathbf{q}^{2h}, \tag{6.2}$$

where $\hat{\mathcal{P}}$ denotes a prolongation operator used by the FMG algorithm for solution interpolation; the "hat" notation is applied to distinguish from the prolongation operator $\mathcal{P}$ used within FAS multigrid cycles for interpolation of coarse-grid corrections. After forming the initial fine-grid solution approximation $\mathbf{q}^h$, a two-level FAS multigrid cycle is applied as following: Several (or perhaps one or even zero) relaxation sweeps are applied to the fine-grid equations to obtain an improved solution approximation $\tilde{\mathbf{q}}^h$. The coarse-grid equations at level $2h$ to be solved for corrections to $\tilde{\mathbf{q}}^h$ are defined as

$$\mathbf{R^{2h}}(\mathbf{q}^{2h}) = \mathbf{R^{2h}}(\hat{\mathcal{R}}\tilde{\mathbf{q}}^h) + \mathcal{R}(\mathbf{f}^h - \mathbf{R^h}(\tilde{\mathbf{q}}^h)), \tag{6.3}$$

where $\hat{\mathcal{R}}$ and $\mathcal{R}$ denote restriction operators for transferring the fine-grid solutions and residuals to the coarse grid, respectively. These coarse-grid equations are then solved by some iterative method (or directly if the

grid is coarse enough). The corrections from the coarse-grid (grid $2h$) solutions are prolonged to the fine grid as

$$\tilde{\mathbf{q}}^h = \tilde{\mathbf{q}}^h + \mathcal{P}(\mathbf{q}^{2h} - \hat{\mathcal{R}}\tilde{\mathbf{q}}^h). \tag{6.4}$$

Several relaxation sweeps follow the coarse-grid correction interpolation to complete one FAS multigrid cycle.

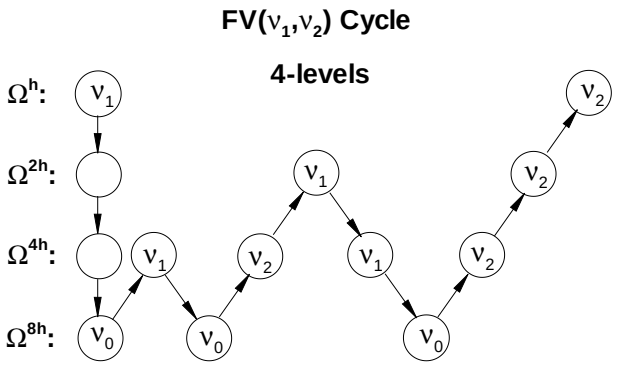


FIG. 6.1. *Schematic of the 4-level $FV(\nu_1, \nu_2)$ cycle, where $\nu_0$ denotes the number of relaxation sweeps on the coarsest mesh and $\Omega^h$ denotes the grid with mesh spacing $h$.*

In multilevel versions of the FAS cycle, the coarse-grid equations are themselves solved with $\gamma$ cycles of the algorithm applied recursively, where $\gamma = 1$ would correspond to a V cycle and $\gamma = 2$ to a W cycle. In our numerical tests, a version of the V cycle, termed FV$(\nu_1, \nu_2)$ cycle, is used. The multilevel FV$(\nu_1, \nu_2)$ cycle has been employed earlier in [24] and is derived from the target-grid two-level FAS cycle described above by applying a multilevel FMG algorithm with the V$(\nu_1, \nu_2)$ cycle to solve the coarse-grid equations. Parameters $\nu_1$ and $\nu_2$ denote the number of relaxation sweeps on the downward and upward legs of the cycle. The cycle is sketched in Figure 6.1.

The distributed relaxation method has been applied as described in Sections 3 and 4. The notations $\mathbf{L_h}$ and $\mathbf{M_h}$ are used below for the principal linearization of the operator $\mathbf{R^h}$ of (6.1) and the corresponding distribution matrix, respectively. The values of auxiliary variables $\delta\mathbf{w}^h$ have been overspecified outside of the computational domain by zeros wherever it is necessary. The convection operators in the $\mathbf{L_h M_h}$ matrix have been solved by downstream marching. The full-potential operator has been relaxed with downstream Gauss-Seidel relaxation sweeps. The inter-grid transfer operators are the following: The prolongation operators, $\hat{\mathcal{P}}$ and $\mathcal{P}$, are the second-order symmetric linear interpolations of the primitive-variable corrections. The operator $\mathcal{R}$ restricting residuals is the second-order full-weighting operator. The solution-restriction operator $\hat{\mathcal{R}}$ is the injection operator.

**7. Numerical Tests.** The results of numerical solutions of nonlinear nonconservative equations corresponding to quasi-one-dimensional subsonic flow in a convergent-divergent channel are reported in this section. The differential equations are (5.1) with $x \in [0, 1]$ and the area distribution term $\sigma(x) = 1 - 0.8x(1 - x)$

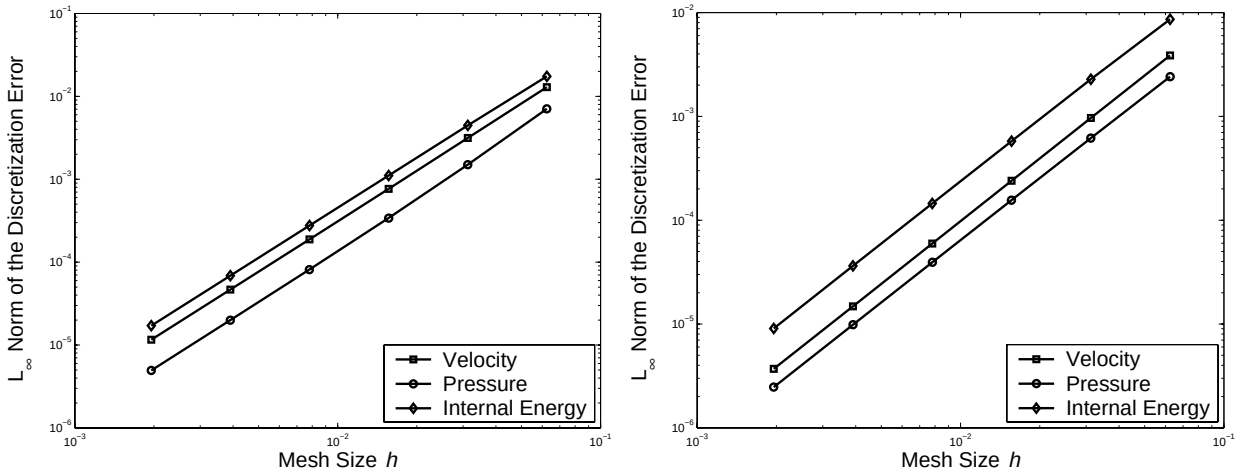


(a) 5-pt full-potential discretization (b) 3-pt full-potential discretization.

FIG. 7.1. *Maximum discretization errors versus grid size.*

Two factorizable discrete schemes approximating (5.1) are tested

$$
\begin{aligned}
u_j^h \partial^u u_j^h + \tfrac{(\gamma-1)\epsilon_j^h}{p_j^h} \partial^c p_j^h &= 0, \\
u_j^h \partial^u \psi_j^h - \mathcal{D}^h p_j^h &= 0, \\
\gamma p_j^h \partial^c u_j^h + \phi_j^h + u_j^h \partial^d p_j^h &= -\gamma p_j^h u_j^h \tfrac{\partial^c \sigma_j^h}{\sigma_j^h}, \\
(\gamma-1)\epsilon_j^h \partial^c u_j^h + u_j^h \partial^u \epsilon_j^h &= -(\gamma-1)\epsilon_j^h u_j^h \tfrac{\partial^c \sigma_j^h}{\sigma_j^h},
\end{aligned}
\tag{7.1}
$$

where $\sigma_j^h = \sigma(jh)$, and

$$
\begin{aligned}
\mathcal{D}_1^h p_j^h &= \tfrac{\gamma(\gamma-1)\epsilon_j^h}{h^2}(p_{j-2}^h - 4p_{j-1}^h + 6 - 4p_{j+1}^h + p_{j+2}^h) \\
&\text{or} \\
\mathcal{D}_2^h p_j^h &= \tfrac{3(u_j^h)^2 + \gamma(\gamma-1)\epsilon_j^h}{4h^2}(p_{j-2}^h - 4p_{j-1}^h + 6 - 4p_{j+1}^h + p_{j+2}^h).
\end{aligned}
\tag{7.2}
$$

TABLE 7.1

*The $L_2$-norm of discretization errors in p and the ratio of algebraic-to-discretization errors for the FMG-1 solver with FV(2,2) cycles.*

| | 5-pt | | 3-pt | |
|---|---|---|---|---|
| $h$ | $\|\|e_d\|\| : p$ | $\|\|e_a\|\|/\|\|e_d\|\| : p$ | $\|\|e_d\|\| : p$ | $\|\|e_a\|\|/\|\|e_d\|\| : p$ |
| 1/32 | 0.6721x$10^{-3}$ | 0.004 | 0.3343x$10^{-3}$ | 0.03 |
| 1/64 | 0.1441x$10^{-3}$ | 0.02 | 0.8585x$10^{-4}$ | 0.01 |
| 1/128 | 0.3579x$10^{-4}$ | 0.02 | 0.2153x$10^{-4}$ | 0.01 |
| 1/256 | 0.8374x$10^{-5}$ | 0.02 | 0.5391x$10^{-5}$ | 0.01 |
| 1/512 | 0.2098x$10^{-5}$ | 0.01 | 0.1350x$10^{-5}$ | 0.01 |

The principal linearization operator and the distribution matrix used in distributed relaxation are one-dimensional versions of (4.4) and (4.5). The discrete equations are solved with an FMG-1 algorithm employing one FV(2, 2) cycle on each grid. The coarsest grid corresponds to $h = 1/16$. The discrete boundary

conditions are overspecified on each grid from the exact differential solution of the fully subsonic flow problem with the inflow Mach number $M = 0.5$. The maximum discretization errors versus mesh size shown in Figure 7.1 demonstrate the second-order spatial convergence. In Table 7.1, the ratios of the algebraic error in the $L_2$-norm to the discretization error in this norm for the FMG-1 algorithm are quite small at each grid. The complexity of this solver is about 30 minimal work units, where a minimal work unit is defined as the number of operations required for one target-grid residual evaluation. The number is relatively large as is typical for one dimension; in two dimensions the complexity of this algorithm would be about 9.3 minimal work units, representing TME according to the definition given at the beginning of the paper.

The residual convergence history versus FV(2,2) multigrid cycles are shown in Figure 7.2. The equations are numbered according to (7.1). The convergence rates are grid-independent and are roughly one order of magnitude per cycle. The discretization with the three-point full-potential factor shows slightly better convergence rates, although, the rates are slightly slower than the asymptotic convergence rate expected if solving only the scalar three-point full-potential equation. Although not shown, the convergence rates somewhat deteriorate when a multigrid V cycle is used instead of the FV cycle.

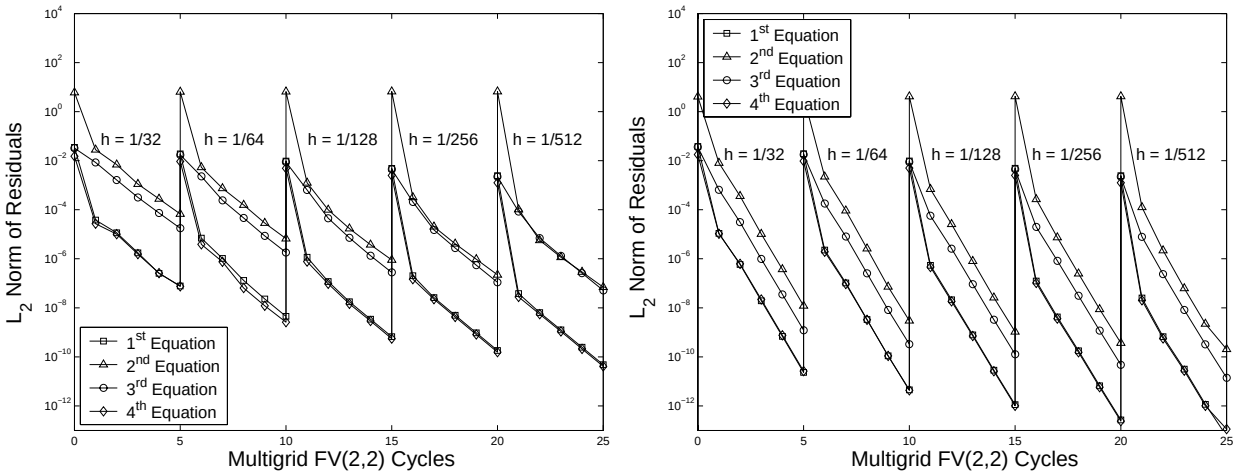


(a) 5-pt full-potential discretization (b) 3-pt full-potential discretization.

FIG. 7.2. *Residual convergence for the FMG algorithm with five FV(2,2) multigrid cycles at each grid level for the nonconservative equations (7.1).*

**8. Concluding Remarks.** A multigrid method is defined as having textbook multigrid efficiency (TME) if solutions to the governing system of equations are attained in a computational work that is a small (less than 10) multiple of the operation count in one target-grid residual evaluation. A way to achieve TME for the Navier-Stokes equations is to apply the distributed relaxation method separating the elliptic and hyperbolic partitions of the equations. Design of a distributed relaxation scheme for the Navier-Stokes systems can be significantly simplified if the target discretization possesses two properties: (1) factorizability and (2) consistent approximations for scalar factors.

The paper has introduced a new family of factorizable discrete schemes for the multidimensional Euler equations. The schemes include a mechanism that allows one to obtain any desired discretization for the full-potential factor of the system determinant without compromising the scheme factorizability. This property opens the door for applying the distributed relaxation technique leading to TME in complicated computational fluid dynamics simulations.

The accuracy of the new schemes has been analyzed, compared with the accuracy of standard schemes, and found competitive. TME and fast grid-independent residual convergence rates have been demonstrated in solution of fully subsonic quasi-one-dimensional flow in a convergent/divergent channel.

**Appendix A. Erratic Convergence of Basic-Scheme Discretization Errors.**

In this appendix, an analysis of discretization errors for the basic scheme (5.20) is presented. This analysis explains both the erratic convergence rates and the mean second-order convergence exhibited by the discretization errors.

Taking the exact solution (5.5) of the differential problem as a Fourier component guarantees that the particular solution (5.24) is a second-order accurate approximation, and that the differences between the solutions converge asymptotically monotonically. Thus, a deviation from the monotonic convergence may occur only because of coefficients $c_k, k = 1, \ldots, 4$, of the characteristic solutions $\mathbf{z}_k$ to the homogeneous problem. For the set of overspecified boundary conditions (5.29), the coefficients $c_k$ are found as

$$\begin{pmatrix} c_1 \\ c_2 \\ c_3 \\ c_4 \end{pmatrix} = \mathbf{T}^{-1} \begin{pmatrix} b_1 \\ b_2 \\ b_3 \\ b_4 \end{pmatrix}, \tag{A.1}$$

where

$$\mathbf{T} = \begin{pmatrix} 1 & 0 & 1 & 1 \\ -\frac{\bar{u}}{2} & \frac{1}{2\rho} & \bar{u}\left(\frac{3}{2}\lambda_3 - 2\right) - \frac{\bar{u}\lambda_3^2 \partial^u(\lambda_3)}{2\partial^c(\lambda_3)} & \bar{u}\left(\frac{3}{2}\lambda_4 - 2\right) - \frac{\bar{u}\lambda_4^2 \partial^u(\lambda_4)}{2\partial^c(\lambda_4)} \\ -\frac{\rho c^2}{2} & \frac{\bar{u}}{2} & -\left(\frac{\rho c^2}{2\lambda_3} + \frac{\rho \bar{u}^2\left(-\frac{3}{2}+2\lambda_3\right)\partial^u(\lambda_3)}{\partial^c(\lambda_3)}\right)\lambda_3^{N-1} & -\left(\frac{\rho c^2}{2\lambda_4} + \frac{\rho \bar{u}^2\left(-\frac{3}{2}+2\lambda_4\right)\partial^u(\lambda_4)}{\partial^c(\lambda_4)}\right)\lambda_4^{N-1} \\ 0 & 1 & \lambda_3^N & \lambda_4^N \end{pmatrix}, \tag{A.2}$$

$$\begin{pmatrix} b_1 \\ b_2 \\ b_3 \\ b_4 \end{pmatrix} = \begin{pmatrix} C_u - \hat{u}^{(1)} \\ -\frac{\bar{u}}{2}\left(C_u - \hat{u}^{(1)}\right) e^{-i\omega} + \frac{1}{2\rho}\left(C_p - \hat{p}^{(1)}\right) \\ \left(-\frac{\rho c^2}{2}\left(C_u - \hat{u}^{(1)}\right) + \frac{\bar{u}}{2}\left(C_p - \hat{p}^{(1)}\right) e^{i\omega}\right) e^{iN\omega} \\ \left(C_p - \hat{p}^{(1)}\right) e^{iN\omega} \end{pmatrix}, \tag{A.3}$$

and $\lambda_3, \lambda_4, \hat{u}^{(1)}$, and $\hat{p}^{(1)}$ are defined in Section 5.1.

All the values $b_k$ converge to zero with second-order rates, and this provides a mean second-order convergence for discretization errors. The determinant of $\mathbf{T}$ is a linear combination of some integer powers (between $-N$ and $N$) of $\lambda_3$. (Recall, that $\lambda_4 = \lambda_3^{-1}$.) The sequence $\lambda_3^N = e^{iN\phi}$ does not converge to any value as $N$ tends to infinity — rather it orbits the unit circle with the frequency determined by $\phi$; $\phi$, in turn, is controlled by the Mach number. Therefore, the determinant of $\mathbf{T}$ is also oscillatory. Theoretically, one could construct a set of boundary conditions and choose the Mach number so that $\mathbf{T}$ degenerates on a particular grid. The discrete problem on this grid would become ill posed. Further grid refinement would unavoidably result in repeating (or closely approaching) ill-posedness on an infinite number of grids. For overspecified boundary conditions, we did not find a Mach number and a grid to enforce the degeneration of the matrix $\mathbf{T}$. However, significant variations of the absolute value of the determinant have been observed.

Figure A.1 presents a convergence history (circle symbols) for the $L_\infty$ norms of discretization errors in pressure. The parameters of the exact solution have been chosen as $C_u = 1, C_p = 2, \alpha = 7\pi$. The Mach

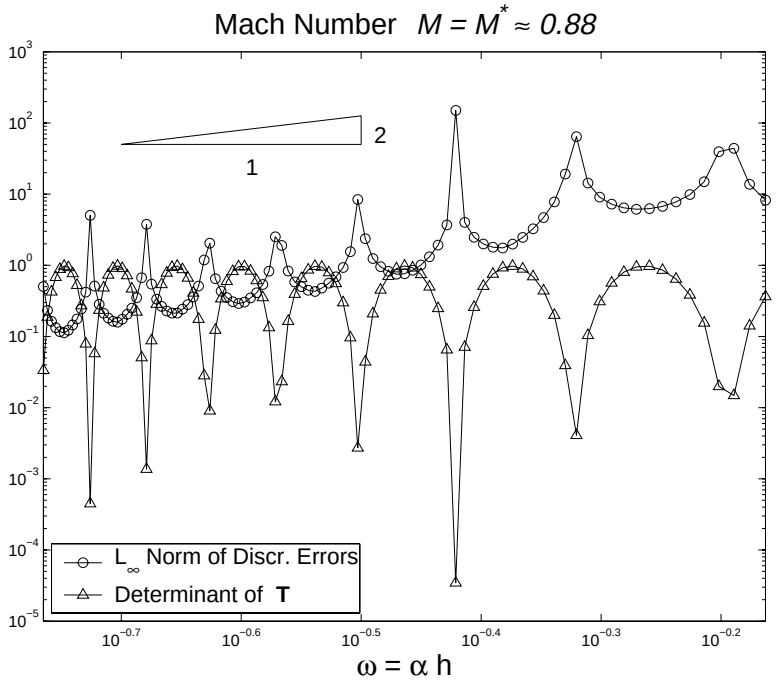


FIG. A.1. *$L_\infty$ norms of discretization errors (circles) and the history of the determinant of* $\mathbf{T}$*(triangles) for the basic discrete scheme with the overspecified boundary conditions.*

number,

$$M^* = \sqrt{\frac{5t^2 + 8 + 8\sqrt{t^2+1}}{25t^2+16}}, \tag{A.4}$$

with $t = \tan(\phi)$, corresponds to $\phi = \pi/4$. The number of grid points has been gradually increased (by 1) rather than doubled in passing to the next fine grid. For comparison, Figure A.1 exhibits the history of the determinant of $\mathbf{T}$ (triangle symbols) as well. The discretization errors do not converge monotonically. Spikes of large discretization errors occur periodically, closely following the pattern of the determinant $\mathbf{T}$ behavior: smaller determinant values correspond to larger discretization errors. A mean second-order convergence rate is observed.

## REFERENCES


[1] S. W. ARMFIELD, *Ellipticity, Accuracy, and Convergence of the Discrete Navier-Stokes Equations*, J. Comput. Phys., 114 (1994), pp. 176–184.

[2] A. BRANDT, *Multigrid solvers for non-elliptic and singular-perturbation steady-state problems.* (unpublished). The Weizmann Institute of Science, Rehovot, Israel, December 1981.

[3] ——, *Guide to multigrid development*, in Multigrid Methods, W. Hackbusch and U. Trottenberg, eds., Lecture Notes in Math. 960, Springer-Verlag, Berlin, 1982.

[4] ——, *Multigrid techniques: 1984 guide with applications to fluid dynamics*, in Lecture Notes for the Computational Fluid Dynamics, Lecture Series at the Von-Karman Institute for Fluid Dynamics, The Weizmann Institute of Science, Rehovot, Israel, 1984. ISBN-3-88457-081-1, GMD-Studien Nr.

85, Available from GMD-AIW, Postfach 1316, D-53731, St. Augustin 1, Germany. Also available from Secretary, Department of Mathematics, University of Colorado at Denver, CO 80204-5300.

[5] ——, *Barriers to achieving textbook multigrid efficiency in CFD*, ICASE Interim Report 32, NASA CR-1998-207647, April 1998. Updated version available as Gauss Center Report WI/GC-10 at The Weizmann Institute of Science, Rehovot, Israel, December 1998.

[6] ——, *Appendix C: Recent developments in multigrid efficiency in computational fluid dynamics*, in Multigrid, Academic Press, London, 2000, pp. 573–589. Ulrich Trottenberg, C. W. Oosterlee, and A. Schüler.

[7] A. Brandt and B. Diskin, *Multigrid solvers for the non-aligned sonic flow: The constant coefficient case*, Computers and Fluids, 28 (1999), pp. 511–549. Also Gauss Center Report WI/GC-8 at The Weizmann Institute of Science, Rehovot, Israel, October 1997.

[8] ——, *Multigrid solvers for nonaligned sonic flows*, SIAM J. Sci. Comp., 21 (2000), pp. 473–501.

[9] A. Brandt, B. Diskin, and J. L. Thomas, *Textbook multigrid efficiency for computational fluid dynamics simulations*, AIAA Paper 2001-2570, 15th AIAA CFD Conference, Anaheim, CA, June 2001.

[10] A. Brandt and S. Ta'asan, *Multigrig solutions to quasi-elliptic schemes*, in Progress and Supercomputing in Computational Fluid Dynamics, E. M. Murman and S. S. Abarbanel, eds., Boston, MA, 1985, Birkhäuser, pp. 143–154.

[11] A. Brandt and I. Yavneh, *On multigrid solution of high-Reynolds incompressible entering flow*, J. Comput. Phys., 101 (1992), pp. 151–164.

[12] ——, *Accelerated multigrid convergence and high-Reynolds recirculating flows*, SIAM J. Sci. Comp., 14 (1993), pp. 607–626.

[13] W. L. Briggs, S. F. McCormick, and V. E.Henson, *Multigrid Tutorial, 2nd edition*, SIAM, USA, 2000.

[14] B. Diskin, *Efficient Multigrid Solvers for the Linearaized Transonic Full Potential Equation*, PhD thesis, The Weizmann Institute of Science, 1998.

[15] B. Diskin and J. L. Thomas, *Distributed relaxation for conservative discretizations*, AIAA Paper 2001-2571, 15th AIAA CFD Conference, Anaheim, CA, June 2001.

[16] C. W. Oosterlee and T. Washio, *Krylov subspace acceleration of nonlinear multigrid with application to recirculating flows*, SIAM J. Scient. Comp., 21(5) (2000), pp. 1670–1690.

[17] T. W. Roberts, *The development of a factorizable multigrid algorithm for subsonic and transonic flow*, AIAA Paper 2001-2572, 15th AIAA CFD meeting, Anaheim, CA, June 2001.

[18] T. W. Roberts, D. Sidilkover, and J. L. Thomas, *Multigrid relaxation of a factorizable conservative discretization of the compressible Euler equations*, June 2000. AIAA Paper 2000-2252.

[19] D. Sidilkover, *Factorizable scheme for the equation of fluid flow*, ICASE Report 99-20, NASA CR-1999-209345, June 1999.

[20] ——, *Some approaches toward constructing optimally efficient multigrid solvers for the inviscid flow equations*, Computers and Fluids, 28 (1999), pp. 551–571.

[21] D. Sidilkover, *Factorizable upwind schemes: The triangular unstructured grid formulation*, AIAA Paper 2001-2575, 15th AIAA CFD meeting, Anaheim, CA, June 2001.

[22] K. Stüben and U. Trottenberg, *Multigrid methods: Fundamental algorithms, model problem analysis and application*, in Multigrid Methods, W. Hackbusch and U. Trottenberg, eds., Lecture Notes in Math. 960, Springer-Verlag, Berlin, 1982, pp. 1–176.

[23] J. L. Thomas, B. Diskin, and A. Brandt, *Distributed relaxation multigrid and defect correction applied to the compressible Navier-Stokes equations*, AIAA Paper 99-3334, 14th Computational Fluid Dynamics Conference, Norfolk, VA, July 1999.

[24] ——, *Textbook multigrid efficiency for the incompressible Navier-Stokes equations: High Reynolds number wakes and boundary layers*, Computers and Fluids, 30 (2001), pp. 853–874. Also ICASE Report 99-51 (NASA CR-1999-209831), December 1999.

[25] J. L. Thomas, B. Diskin, A. Brandt, and J. C. South, *General framework for achieving textbook multigrid efficiency: Quasi-1-d Euler example*, in Frontiers of Computational Fluid Dynamics — 2002, D. A. Caughey and M. M. Hafez, eds., World Scientific Publishing Company, Singapore, 2002, pp. 61–79. Also ICASE Report 2000-30, NASA/CR-2000-210320.

[26] U. Trottenberg, C. W. Oosterlee, and A. Schüler, *Multigrid*, Academic Press, London, 2000.

[27] P. Wesseling, *An introduction to multigrid methods*, Pure and Applied Mathematics, John Wiley & Sons, Chichester, 1992.

[28] I. Yavneh, C. Venner, and A. Brandt, *Fast multigrid solution of the advection problem with closed characteristics*, SIAM J. Sci. Comp., 19 (1998), pp. 111–125.

# REPORT DOCUMENTATION PAGE

*Form Approved*
*OMB No. 0704-0188*



| 1. AGENCY USE ONLY *(Leave blank)* | 2. REPORT DATE | 3. REPORT TYPE AND DATES COVERED |
|---|---|---|
| | April 2002 | Contractor Report |

**4. TITLE AND SUBTITLE**
New factorizable discretizations for the Euler equations

**5. FUNDING NUMBERS**
C NAS1-97046
WU 505-90-52-01

**6. AUTHOR(S)**
Boris Diskin and James L. Thomas

**7. PERFORMING ORGANIZATION NAME(S) AND ADDRESS(ES)**
ICASE
Mail Stop 132C
NASA Langley Research Center
Hampton, VA 23681-2199

**8. PERFORMING ORGANIZATION REPORT NUMBER**
ICASE Report No. 2002-6

**9. SPONSORING/MONITORING AGENCY NAME(S) AND ADDRESS(ES)**
National Aeronautics and Space Administration
Langley Research Center
Hampton, VA 23681-2199

**10. SPONSORING/MONITORING AGENCY REPORT NUMBER**
NASA/CR-2002-211456
ICASE Report No. 2002-6

**11. SUPPLEMENTARY NOTES**
Langley Technical Monitor: Dennis M. Bushnell
Final Report
To be submitted to the SIAM Journal on Scientific Computing.

**12a. DISTRIBUTION/AVAILABILITY STATEMENT**
Unclassified–Unlimited
Subject Category 64
Distribution: Nonstandard
Availability: NASA-CASI (301) 621-0390

**12b. DISTRIBUTION CODE**

**13. ABSTRACT** *(Maximum 200 words)*
A multigrid method is defined as having textbook multigrid efficiency (TME) if solutions to the governing system of equations are attained in a computational work that is a small (less than 10) multiple of the operation count in one target-grid residual evaluation. A way to achieve TME for the Euler and Navier-Stokes equations is to apply the distributed relaxation method thereby separating the elliptic and hyperbolic partitions of the equations. Design of a distributed relaxation scheme can be significantly simplified if the target discretization possesses two properties: (1) factorizability and (2) consistent approximations for the separate factors. The first property implies that the discrete system determinant can be represented as a product of discrete factors, each of them approximating a corresponding factor of the determinant of the differential equations. The second property requires that the discrete factors reflect the physical anisotropies, be stable, and be easily solvable.

In this paper, discrete schemes for the nonconservative Euler equations possessing properties (1) and (2) have been derived and analyzed. The accuracy of these schemes has been tested for subsonic flow regimes and is comparable with the accuracy of standard schemes. TME has been demonstrated in solving fully subsonic quasi-one-dimensional flow in a convergent/divergent channel.

**14. SUBJECT TERMS**
Euler equations, textbook multigrid efficiency, distributed relaxation, factorizable schemes

**15. NUMBER OF PAGES**
27

**16. PRICE CODE**
A03

| 17. SECURITY CLASSIFICATION OF REPORT | 18. SECURITY CLASSIFICATION OF THIS PAGE | 19. SECURITY CLASSIFICATION OF ABSTRACT | 20. LIMITATION OF ABSTRACT |
|---|---|---|---|
| Unclassified | Unclassified | | |